Spectra of double-cumulative photons in the central rapidity region at high transverse momenta

Article *in* Physics of Atomic Nuclei · November 2015

DOI: 10.1134/S1063778815070029

CITATIONS
2

READS
71

16 authors, including:

A. A. Golubev
Institute for Theoretical and Experimental Physics
171 PUBLICATIONS **1,378** CITATIONS
SEE PROFILE

V. S. Goryachev
Institute for Theoretical and Experimental Physics
25 PUBLICATIONS **537** CITATIONS
SEE PROFILE

Natalia Mikhaylovna Zhigareva
Institute for Theoretical and Experimental Physics
136 PUBLICATIONS **6,349** CITATIONS
SEE PROFILE

Sergey Mikhajlovich Kiselev
CERN
14 PUBLICATIONS **104** CITATIONS
SEE PROFILE

ISSN 1063-7788, Physics of Atomic Nuclei, 2015, Vol. 78, No. 8, pp. 936–942. © Pleiades Publishing, Ltd., 2015.
Original Russian Text © I.G. Alekseev, A.A. Golubev, V.S. Goryachev, G.B. Dzubenko, A.G. Dolgolenko, N.M. Zhigareva, S.M. Kiselev, K.R. Mikhaylov, E.A. Morozova, P.A. Polozov, M.S. Prokudin, D.V. Romanov, D.N. Svirida, A.V. Stavinsky, V.L. Stolin, G.B. Sharkov, 2015, published in Yadernaya Fizika, 2015, Vol. 78, No. 11, pp. 995–1001.

ELEMENTARY PARTICLES AND FIELDS
Experiment

Spectra of Double-Cumulative Photons in the Central Rapidity Region at High Transverse Momenta[1)]

I. G. Alekseev, A. A. Golubev, V. S. Goryachev, G. B. Dzubenko, A. G. Dolgolenko, N. M. Zhigareva, S. M. Kiselev, K. R. Mikhaylov*, E. A. Morozova, P. A. Polozov, M. S. Prokudin, D. V. Romanov, D. N. Svirida, A. V. Stavinsky, V. L. Stolin, and G. B. Sharkov

Institute for Theoretical and Experimental Physics, National Research Center Kurchatov Institute, Bol'shaya Cheremuskinskaya ul. 25, Moscow, 117218 Russia

Received April 10, 2015

Abstract—The spectra of photons produced in the interaction between carbon ions of kinetic energy 2.0 and 3.2 GeV per nucleon and beryllium nuclei were measured at the FLINT facility by means of electromagnetic calorimeters that is deployed at the accelerator of the Institute for Theoretical and Experimental Physics (ITEP, Moscow). The spectra in question were measured in the central rapidity region (at angles between 35° and 73° in the laboratory frame) at photon energies of 1 to 3 GeV by using a cumulative-photon trigger. An analysis of the data obtained in this way reveals that the interaction of multinucleon fluctuation in the projectile nucleus with a multinucleon fluctuation in the target nucleus is a dominant process that leads to photon production in the measured region of angles and momenta. As a development of the generally accepted terminology, an interaction of this type may be called a double cumulative interaction.

DOI: 10.1134/S1063778815070029

INTRODUCTION

Investigations into cumulative processes discovered at the Institute for Theoretical and Experimental Physics (ITEP, Moscow) and at the Institute for High Energy Physics (IHEP, Protvino) [1, 2] and vigorously studied since the mid-1970s yielded a number of interesting results and led to establishing basic regularities of cumulative processes (see, for example, [3, 4]). Yet, there is still no consensus on the mechanism of cumulative-particle production. To a considerable extent, this is due to the scarcity of correlation data. However, there is no doubt among the physics community about the presence of a new phenomenon in the whole set of accumulated data. The presence of local multinucleon correlations (fluctons according to the terminology proposed by Blokhintsev [5]) in nuclei is usually employed in one form or another to explain this phenomenon. Experimental data indicate that the properties of fluctons are similar to a considerable extent to the presumed properties of cold superdense matter, but it is of course illegitimate to identify directly fluctons, which are obviously nonequilibrium objects, with droplets of superdense matter. The answer to the question of whether such an identification with a final state that originates from the interaction with a flucton is possible is not so obvious. A comparatively small number of nucleons in a "droplet" is the main problem here. Therefore, it is highly desirable to extend experiments to the region of the maximum accessible cumulative order and to retain simultaneously the scale of momentum (velocity according to Baldin's terminology) transfers in the interaction at the current level. This task becomes especially important in view of the development of theoretical ideas of the phase diagram of nuclear matter at high baryon densities [6]. Maximum cumulative orders reached in proton–nucleus collisions are three to four [7]. It is extremely difficult to go farther along these lines, since, according to CLAS data [8], the probability for observing a three-nucleon correlation is lower than the square of the probability for observing a two-nucleon fluctuation. Of course, higher cumulative orders may formally be reached in fragment emission from nuclei, but this path seems hardly promising for obtaining dense "droplets" whose char-

*E-mail: kmikhail@itep.ru

1) This article was written on the basis of a report presented at the conference Physics of Fundamental Interactions held at the Institute for Theoretical and Experimental Physics (ITEP, Moscow, Russia) in November 21–25, 2011, during a session of Nuclear Physics Section at the General Physics Department, Russian Academy of Sciences.

acteristic size is on an hadronic scale. Indeed, fragments as such have dimensions characteristic of nuclei rather than of nucleons. Searches for flucton–flucton interaction in collisions of two nuclei is more promising in our opinion, since this gives grounds to hope for the doubling of the number of nucleons in the product "droplet" and should in principle permit reaching a cumulative order of seven to eight at the level of cross sections accessible in present-day experiments. In this article, we report on new results of the FLINT experiment [9, 10], which performs searches for flucton–flucton interaction characterized by the maximum possible cumulative order.

EXPERIMENTAL PROCEDURE USED

Our experiment was performed in the magnetic hall of the ITEP accelerator complex. The layout of the experimental setup used is shown in Fig. 1. Carbon nuclei accelerated to a kinetic energy of 2.0 GeV per nucleon in one exposure and to a kinetic energy of 3.2 GeV per nucleon in the other exposure interacted with a beryllium-foil target introduced in the ring of the ITEP synchrotron. Electromagnetic calorimeters based on F8 lead glasses and grouped into two supermodules each containing 64 glasses were arranged at angles in the range of 35°–73° (in the laboratory frame) at a distance of 2.6 m on average from the target. The dimensions of each glass were $100 \times 100 \times 380$ mm. The properties of the glasses and the structure of the supermodules were described in [10].

The intensity of the carbon beam was at a level of 10^8 ions per accelerator cycle every four seconds. The spill duration was about 0.5 s. The efficiency of the inner beryllium target was estimated at 5%. The beam-quality control was executed with the aid of a monitor consisting of four identical scintillation detectors connected in line. These detectors formed a telescope directed to the target. The monitor was oriented at an angle of 90° with respect to the beam and was positioned at a distance of 2 m from the beryllium target.

Some events were processed in an on-line mode. This made it possible to test the quality of accumulated data and to find out whether the thresholds set for the trigger were optimal. In the presence of a trigger signal (which was generated if the amplitude of the signal in one of the glasses corresponded to a photon of energy above 1 GeV for emission angles larger than 55° and above 2 GeV for emission angle smaller than 53°), the amplitude was digitized by a flash analog-to-digital converter (ADC) and was saved in a buffer, whereupon information about the magnitude, shape, and arrival time of signals from all 128 glasses of the calorimeter was read out into a database. In order to test the performance of the setup and to control the stability of its parameters, all modules of the calorimeter were tested with photodiode signals with a frequency of 10 Hz. In all, we accumulated about 10 million events satisfying the chosen trigger.

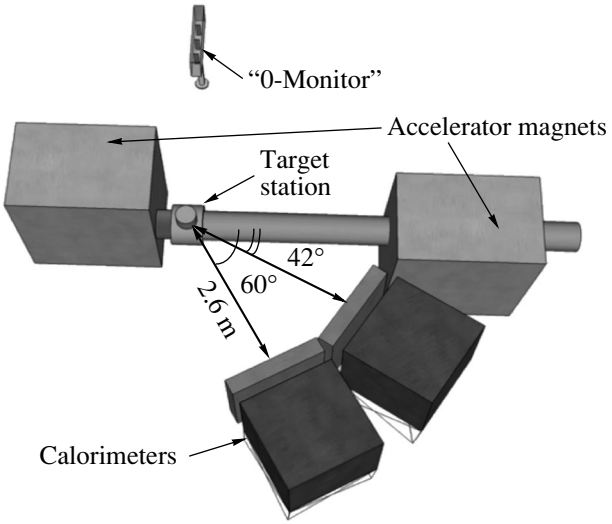

Fig. 1. Layout of the FLINT setup in the present experiment.

PROCESSING AND ANALYSIS OF EXPERIMENTAL DATA

The data-acquisition system developed at ITEP [11] is implemented in the VME standard. It involves performing an analog-to-digital conversion of signals from the detectors, saving relevant information in a buffer, and transferring this information to storing disks via the Ethernet network (the interested reader can find a description of the FLINT data-acquisition system in [10]). An efficient data analysis aimed at removing background signals becomes possible owing to digitizing signals with the aid of a flash ADC.

The cross-sectional area of the lead glasses employed in the calorimeters is 100×100 mm. Owing to the use of a cumulative-photon trigger and the fact that the glass dimensions substantially are larger than the Molière radius (38 mm), a major part of a photon shower is detected within a single calorimeter module. This is because the angular dependence of the cross section for cumulative-photon production is quite smooth, while its energy dependence has an exponential character. The shower being considered basically spreads to only one neighboring glass. We have analyzed the change in the slope of the spectrum versus the threshold for the magnitude of the signal in the neighboring glass (fragment) where it was maximal among the glasses surrounding the central

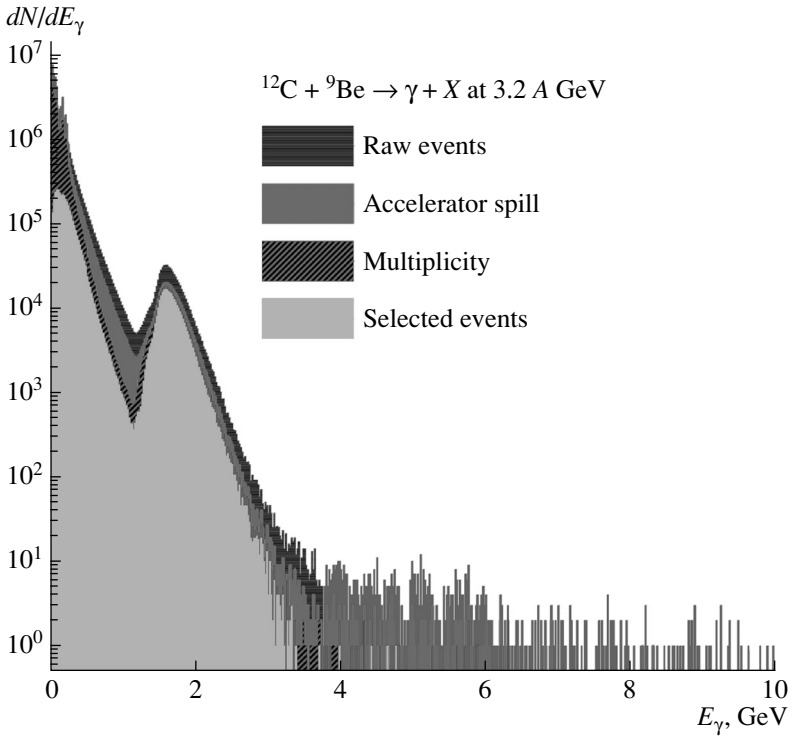

Fig. 2. Energy spectrum of photons that was integrated with respect to the emission angle (between 35° and 53°) in individual calorimeter module at the primary energy of 3.2 GeV per nucleon.

glass. This analysis revealed that, as the threshold for the fragment fraction decreases from 25% to 10%, the slope of the spectrum changes by not more than 5%. The spectra presented in this article were obtained with a threshold less than 15% for the fragment fraction. In the following, we identify the shower energy deposition in one calorimeter module with the total photon energy.

The integrated amplitude spectrum in an individual calorimeter module is shown in Fig. 2 upon transforming it into the energy spectrum with allowance for the results of calibration measurements. Data in Fig. 2 refer to the initial kinetic energy of 3.2 GeV per nucleon and emission angles in the range of 35°–53°. Several characteristic regions can be singled out in this spectrum. A peak in the region around 2 GeV is due to events corresponding to the case where a signal in which the maximum value of the amplitude exceeds the preset trigger threshold is detected in the calorimeter module being considered. This peak is broad since the relationship between the amplitude at the maximum and the integral in question is ambiguous. The part of the spectrum in the region extending to the energy of 1 GeV is the spectrum of signals in the module under study in the case where the trigger was formed by another calorimeter module. An approximately exponential character of the spectrum in the energy range between 2 and 3 GeV gives way to a weaker decrease at higher energies. In order to clarify the nature of this flattening, we applied a system of three kinds of cuts: those on the quality of the beam dump onto the target, on the multiplicity of signals in the calorimeters, and on the signal shape. The results of successively applying these cuts are also given in Fig. 2. One can see that the majority of events in the energy region above 3 GeV do not meet the chosen criteria of a "good" event. After the application of all three criteria, the spectrum becomes close in shape to an exponential spectrum over the whole region of energies above 2 GeV. Among useful events, a moderately small fraction of about 40%, which depends only slightly on the photon energy was lost as the result of applying the above selections. This seems a reasonable price for suppressing the background by more than one order of magnitude.

RESULTS AND DISCUSSION

The photon energy spectra measured at various values of the emission angle are shown in Fig. 3 for the primary kinetic energy of 2.0 GeV per nucleon and in Fig. 4 for the primary kinetic energy of 3.2 GeV per nucleon. One can see that the spectra in question have an exponential character and that the cross sections and slope parameters decrease with increasing photon emission angle and increase with

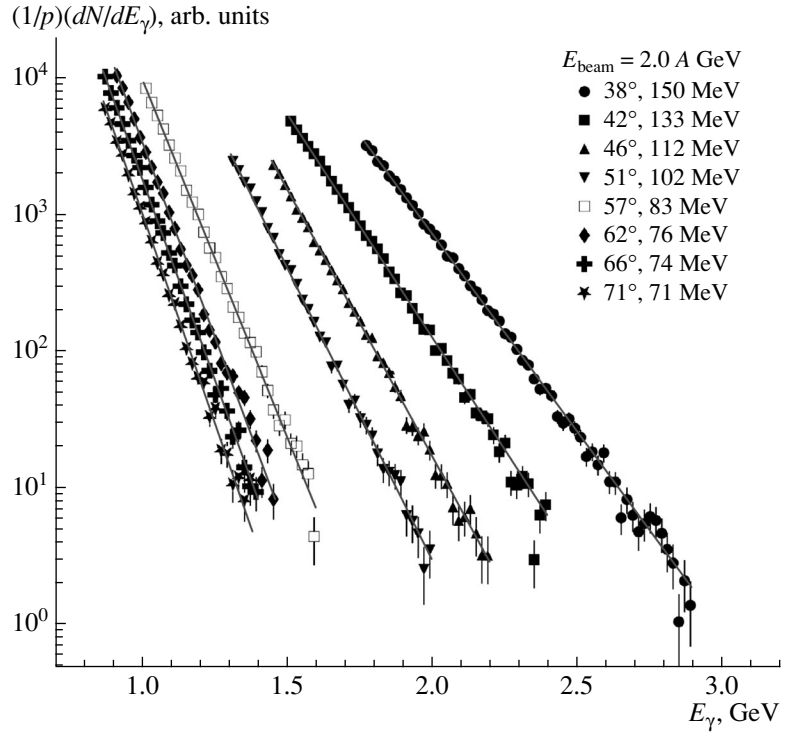

Fig. 3. Photon spectra in the reaction C + Be → $\gamma + X$ at the energy of 2.0 GeV per nucleon for various values of the photon emission angle.

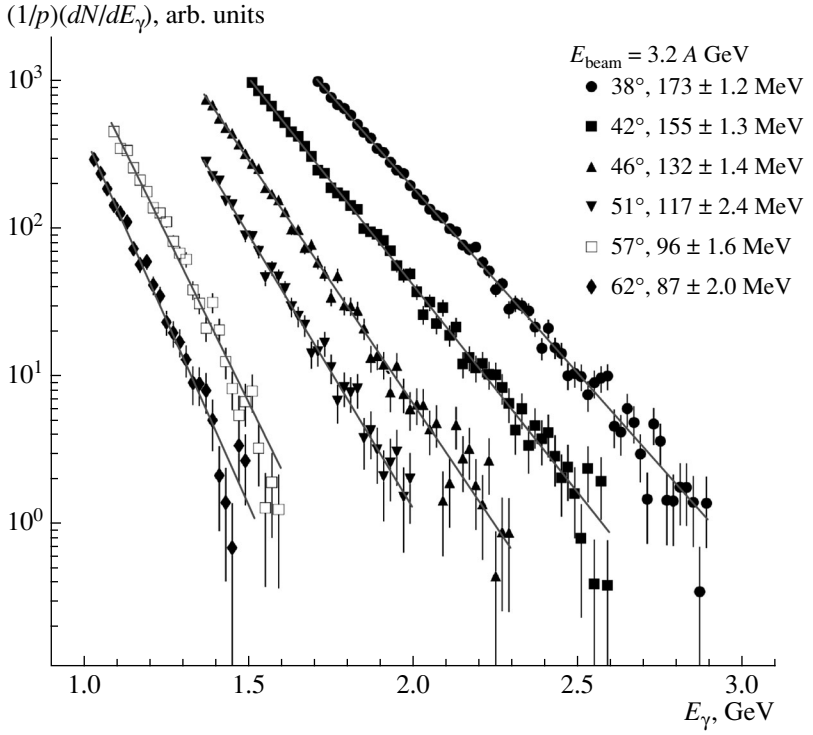

Fig. 4. Photon spectra in the reaction C + Be → $\gamma + X$ at the energy of 3.2 GeV per nucleon for for various values of the photon emission angle.

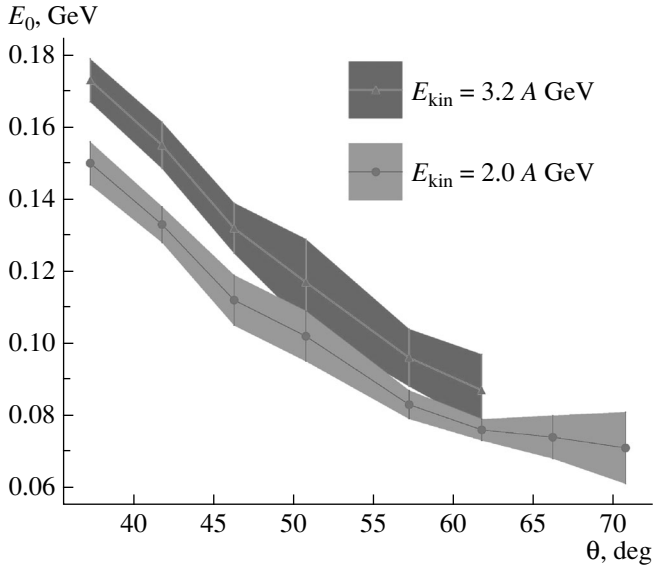

Fig. 5. Slope of the spectrum $[1/p \cdot dN/dE$ was approximated by the function const $\cdot \exp(-E/E_0)]$ as a function of the angle and primary energy.

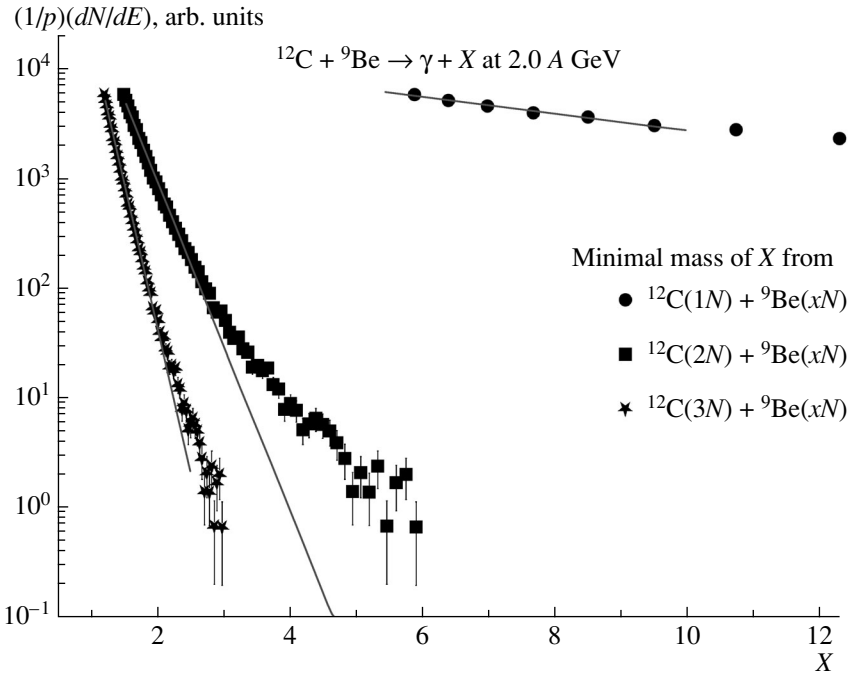

Fig. 6. Photon spectrum measured in the reaction C + Be $\rightarrow \gamma + X$ at the energy of 2.0 GeV per nucleon and integrated with respect to the emission angle over the range of $35^\circ - 53^\circ$ versus the cumulative number X.

increasing primary energy. The results of approximating the spectra by exponential dependences are given in Fig. 5. The scale of the slope parameters of the spectra (about m_π) is of importance for obtaining deeper insight into the character of the interaction that produces these photons. This is a scale that is characteristic of cumulative processes and which lies in the region of energies far from the absolute kinematical boundaries for interacting nuclei as a discrete unit. A sizable primary-energy dependence of the spectra is natural for the region of secondary-particle energies commensurate with the energy per nucleon of the primary nucleus. The emission-angle dependence is also natural at a qualitative level because of the motion of the center-of-mass frame.

In order to understand the character of the inter-

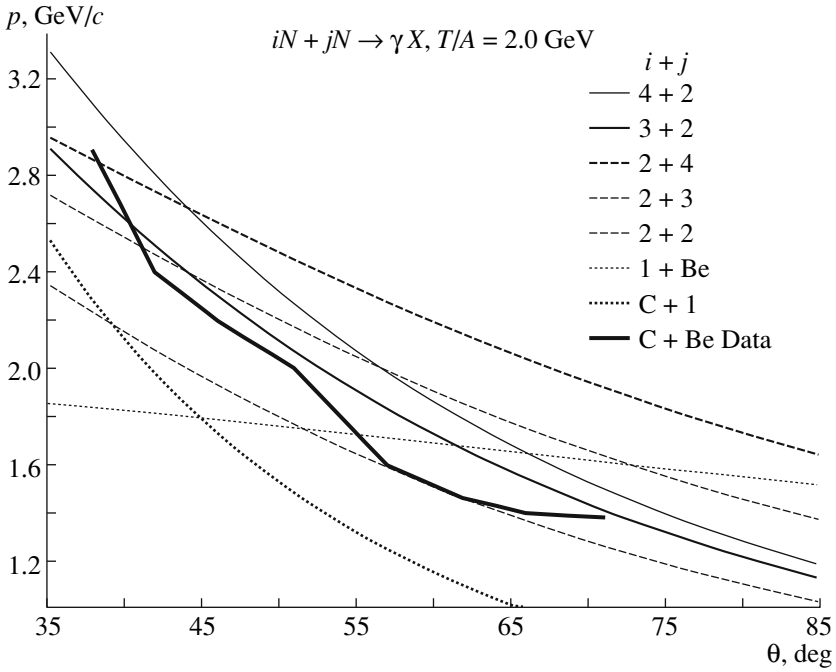

Fig. 7. Kinematical boundaries for hypothetically selected subprocesses of the interaction between N_b nucleons of the projectile nucleus of energy 2.0 GeV per nucleon and N_t target nucleons.

action, we present in Fig. 6 the dependence of the photon spectrum in the reaction C + Be $\to \gamma + X$ at the energy of 2 GeV per nucleon on the cumulative number X (this spectrum was integrated over the angular range of $35°-53°$),

$$Xm_N = \frac{E_0E - p_0p\cos\theta - m^2/2}{T_0 - E}, \qquad (1)$$

where E_0, p_0, and T_0 are the projectile primary energy, momentum, and kinetic energy, respectively, while E, p, θ, and m are respectively, the energy, momentum, emission angle, and mass of the product particle. We calculated the cumulative number for three hypotheses: that of nucleon–flucton interaction, that of flucton–flucton interaction involving two nucleons from the carbon projectile nucleus, and flucton–flucton interaction involving three nucleons of the carbon projectile nucleus. Figure 6 shows that, within the first hypothesis, a major part of measured points of the spectrum lie beyond the kinematical boundary for the beryllium nucleus as a discrete unit ($X = 9$). Within the second hypothesis, the whole spectrum lies in the region of cumulative numbers between 2 and 6. Here, one can see a break point in the spectrum around $X = 3$. Within the third hypothesis, the whole spectrum lies in the region of cumulative numbers between 1 and 3. There is still a break point in the spectrum in this case inclusive, but it is not as pronounced as within the second hypothesis. Upon formally approximating the spectrum within these hypotheses by a function of the form const $\cdot \exp(-X/X_0)$, we arrive at $X_0 = 5.6$ within the first hypothesis, $X_0 = 0.29$ within the second hypothesis, and $X_0 = 0.16$ within the third hypothesis (this value is in fairly good agreement with the slope of the spectrum of cumulative particles [7, 12]). On the basis of these naive ideas, one can see that the third hypothesis is the most reasonable.

In order to give a clear idea of the kinematical region in which we measured photon spectra, the kinematical boundaries (the highest possible photon energies at a given emission angle) are presented in Fig. 7 for hypothetically selected subprocesses of the interaction between N_b nucleons belonging to a projectile nucleus of kinetic energy 2.0 GeV per nucleon and N_t target nucleons (the motion of the chosen nucleon groups within the nuclei involved is not considered). The upper boundary of the measured spectra as a function of the photon emission angle is also shown here. It can be seen that the spectra in question were measured far beyond the boundaries of nucleon–nucleon (NN) interaction (the "standard" Fermi motion of nucleons shifts the boundaries of the region allowed for NN interaction, but this shift is insignificant in relation to the scale over which the spectra under discussion go beyond the NN boundaries). The introduction of a "nonstandard" momentum distribution of nucleons in a nucleus is sometimes used to explain the measured spectra of cumulative particles, but no heuristic value of this has so

far been revealed. As a matter of fact, this is nothing but an alternative representation of data. Moreover, the nature of the Fermi momentum is associated with Fermi statistics of nucleons. A group that contains an even number of nucleons cannot have a half-integer spin and therefore should not obey Fermi statistics. The minimum number of nucleons that should be involved in the interaction from the two nuclei for the entire body of the data obtained to be explained is six. It should be noted that this value is reached only in the case where, in both colliding nuclei, more than one nucleon are involved in the interaction. Obviously, this corresponding to flucton–flucton interaction. The inclusion of only flucton–nucleon and nucleon–flucton interaction does not seem sufficient for a number of reasons. It is well known that an increase of one unit in the cumulative order leads to a decrease in the cross section by two to three orders of magnitude. Since the addition of one nucleon extends, in our case, the kinematical boundaries of nucleon–flucton interaction by a value as small as about 100 MeV, the expected slope of the spectrum would then be about 20 MeV (with allowance for the calorimeter energy resolution, which is about 30 MeV), but this is severalfold smaller than the measured slope parameter. The summed minimal number of nucleons that is necessary for explaining our data within the hypothesis of nucleon–flucton (flucton–nucleon) interaction is substantially greater than that within the hypothesis of flucton–flucton interaction. This means that their expected contribution is several order of magnitude smaller than the contribution of flucton–flucton interaction. Finally, we note that, among measured points, there are those that go beyond the kinematical boundaries of pBe and Cp interactions.

CONCLUSIONS

On the basis of our results, we can draw the following conclusions. At the upgraded FLINT setup, we have measured photon spectra in the reaction $\mathrm{C} + \mathrm{Be} \to \gamma + X$ at the projectile kinetic energies of 2.0 and 3.2 GeV per nucleon over a broad angular range. The photon energy spectra have an exponential form. The slope of the spectra depends on the primary energy and on the photon emission angle. A preliminary analysis of our data reveals that protons originate from flucton–flucton interaction.

ACKNOWLEDGMENTS

This work was supported by the Rosatom State Nuclear Energy Corporation and the Russian Foundation for Basic Research (project nos. 14-02-93107, 14-02-93108, and 14-02-00896).

We are grateful to the personnel of the ITEP accelerator complex for ensuring a stable performance of the accelerator in the course of our experiment.

REFERENCES

1. A. M. Baldin et al., Sov. J. Nucl. Phys. **18**, 41 (1974).
2. Yu. D. Bayukov et al., Sov. J. Nucl. Phys. **18**, 639 (1974).
3. V. S. Stavinskii, Sov. J. Part. Nucl. **10**, 373 (1979).
4. V. B. Gavrilov and G. A. Leksin, Preprint ITEF-37 (Inst. Theor. Exp. Phys., Moscow, 1990).
5. D. I. Blokhintsev, Sov. Phys. JETP **6**, 995 (1958).
6. L. McLerran, arXiv:1105.4103 [hep-ph].
7. S. V. Boyarinov et al., Sov. J. Nucl. Phys. **46**, 871 (1987).
8. K. S. Egiyan et al., Phys. Rev. Lett. **96**, 082501 (2006).
9. I. G. Alekseev, V. E. Vishnyakov, A. I. Golutvin, V. S. Goryachev, G. B. Dzubenko, A. G. Dolgolenko, B. V. Zagreev, S. M. Kiselev, I. E. Korolko, G. A. Leksin, K. R. Mikhaylov, P. A. Polozov, M. S. Prokudin, D. N. Svirida, A. V. Stavinsky, V. L. Stolin, and G. B. Sharkov, Phys. At. Nucl. **71**, 1848 (2008).
10. I. G. Alekseev, S. G. Belogurov, V. E. Vishnyakov, A. I. Golutvin, V. S. Goryachev, G. B. Dzyubenko, A. G. Dolgolenko, B. V. Zagreev, S. M. Kiselev, I. E. KorolTko, I. F. Larin, G. A. Leksin, K. R. Mikhailov, P. A. Polozov, M. S. Prokudin, et al., Instrum. Exp. Tech. **51**, 491 (2008).
11. Spartan-II 2.5V FPGA Complete Data Sheet. http://www.xilinx.com
12. Yu. D. Bayukov, Sov. J. Nucl. Phys. **50**, 638 (1989).